

# Vortex Ordering and Dynamics on Santa Fe Artificial Ice Pinning Arrays

Wenzhao Li,<sup>1</sup> C. J. O. Reichhardt,<sup>2, a)</sup> B. Jankó<sup>1</sup>, and C. Reichhardt<sup>2</sup>

<sup>1)</sup>Department of Physics, University of Notre Dame, Notre Dame, Indiana 46656

<sup>2)</sup>Theoretical Division and Center for Nonlinear Studies, Los Alamos National Laboratory, Los Alamos, New Mexico 87544

(Dated: 29 January 2021)

We numerically examine the ordering, pinning and flow of superconducting vortices interacting with a Santa Fe artificial ice pinning array. We find that as a function of magnetic field and pinning density, a wide variety of vortex states occur, including ice rule obeying states and labyrinthine patterns. In contrast to square pinning arrays, we find no sharp peaks in the critical current due to the inherent frustration effect imposed by the Santa Fe ice geometry; however, there are some smoothed peaks when the number of vortices matches the number of pinning sites. For some fillings, the Santa Fe array exhibits stronger pinning than the square array due to the suppression of one-dimensional flow channels when the vortex motion in the Santa Fe lattice occurs through the formation of both longitudinal and transverse flow channels.

## I. INTRODUCTION

In an artificial spin ice (ASI) system<sup>1,2</sup> the states can be effectively described as spin-like degrees of freedom which can obey the same ice rules found for the ordering of protons in water ice<sup>3</sup> or of atomic spins in certain materials<sup>4,5</sup>. One of the first artificial spin ice systems was constructed from coupled magnetic islands in which the magnetic moment of each island can be described as a single classical spin<sup>1,6</sup>. In this system, for specific arrangements of the effective spins at the vertices, the ground state obeys the ice rules and a vertex at which four spins meet has two spins pointing 'in' and two spins pointing 'out'. Configurations that obey the ice rule can have long range order, such as in square ice<sup>1,6-8</sup>, or they can be disordered, such as in kagomé ice<sup>1,9</sup>. A wide range of additional geometries beyond square and kagomé ice have been proposed<sup>2,10</sup> and realized<sup>11-15</sup>, including mixed geometries which force the formation of excited vertices<sup>10,11,16</sup>.

In addition to studies in magnetic ASI systems, there are several particle-based realizations of ASI<sup>17</sup>, where a collection of interacting particles is coupled to some form of substrate to create states that obey the ice rules. Such systems have been studied for colloidal particles coupled to ordered substrates<sup>18-22</sup>, magnetic skyrmions<sup>23</sup>, and vortices in type-II superconductors with nanostructured pinning arrays<sup>24-30</sup>. The ice rule obeying states often arise through different mechanisms in the particle-based systems compared to magnetic ice systems, since the particle ices minimize Coulomb energy rather than vertex energy<sup>21,31</sup>. In this work we consider vortices interacting with a variation of the ASI geometry which is called a Santa Fe spin ice.

Santa Fe (SF) spin ice, shown in Fig. 1(a), can contain both frustrated and non-frustrated vertices<sup>10,16,32</sup>, forcing some vertices to be in an excited state. In the particle-based model, this would mean that some fraction of the particles are close together, whereas the ground state of a square ice array does not include such close particle spacings. In superconducting ASI systems with non-frustrated ground states, a series

of peaks appear in the critical current at the fields corresponding to ice rule obeying states as well as at higher matching fields<sup>25,26,28</sup>.

In this paper, we use numerical simulations to investigate the vortex configurations, pinning, and flow patterns in a system with a Santa Fe ASI geometry. We find numerous distinct vortex patterns for increasing magnetic field or different pinning densities. At the half matching field, the vortex configurations are close to those expected for the ground state of the SF ice. Compared to the square pinning lattice, in the SF ice we find only weak or smeared peaks in the critical depinning current, and we show that the vortex flow patterns are much more disordered. For dense pinning arrays, the ice rule obeying states vanish but the vortices form a labyrinthine pattern.

## II. SIMULATION

We consider a two-dimensional system of  $N_v$  vortices interacting with an ordered array of pinning sites which are placed either in a Santa Fe artificial spin ice pattern or in a square lattice. The system contains  $N_p$  pinning sites. The number of vortices is proportional to the applied magnetic field  $B$ , and  $N_v = N_p$  corresponds to the matching condition  $B/B_\phi = 1.0$ , where  $B_\phi$  is the matching field. There are periodic boundary conditions in the  $x$  and  $y$ -directions and the equation of motion for a vortex  $i$  is given by

$$\eta \frac{d\mathbf{R}}{dt} = \mathbf{F}_i^{vv} + \mathbf{F}_i^p + \mathbf{F}^d. \quad (1)$$

The damping constant  $\eta$  is set to unity. The vortex-vortex interactions are repulsive and given by  $\mathbf{F}_i^{vv} = \sum F_0 K_1(R_{ij}/\lambda) \hat{\mathbf{R}}_{ij}$ , where  $K_1$  is the modified Bessel function,  $R_{ij}$  is the distance between vortex  $i$  and vortex  $j$ , and  $F_0 = \phi_0^2/2\pi\mu_0\lambda^3$ . We set the penetration depth to  $\lambda = 1.8$ . In the absence of pinning sites, the vortices form a triangular lattice. A uniform driving force  $\mathbf{F}^d = F^d \hat{\mathbf{x}}$  is applied to all the vortices, and the system is considered depinned when the average steady-state vortex velocity is larger than a non-trivial value.

The pinning sites are modeled as localized traps of radius  $r_p$  with the form  $F_i^p = -\sum_1^{N_p} F_p R_{ik} \exp(-R_{ik}^2/r_p^2) \hat{\mathbf{R}}_{ik}$  where  $R_{ik}$  is

<sup>a)</sup>Electronic mail: cjr@lanl.gov

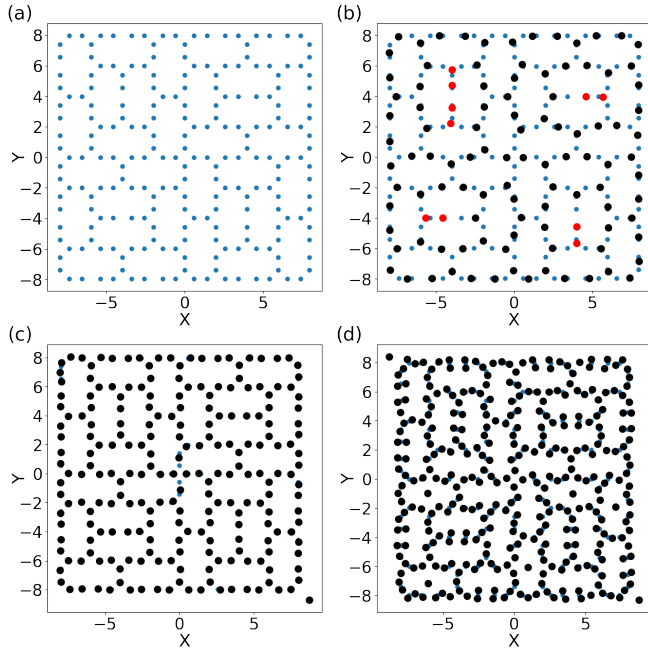


FIG. 1. (a) Blue dots indicate the pinning sites arranged in a Santa Fe ASI geometry with  $d = 0.825$ . (b) The vortex positions (black dots) and pinning locations (blue dots) for the system in panel (a) at  $B/B_\phi = 1/2$ , where the ice rule is mostly obeyed but there are scattered excitations present (red dots). (c)  $B/B_\phi = 1.0$ . (d)  $B/B_\phi = 1.5$ .

the distance between vortex  $i$  and pin  $k$ , and we set  $r_p = 0.6$ . We match our system geometry to the experiments on square vortex ice systems<sup>25</sup>, where  $d$  is the distance between two pinning sites. In Fig. 1(a) we show an example of a Santa Fe pinning array containing four cells. Each cell is divided into eight elementary rectangular plaquettes in which the pinning sites can be grouped into pairs that are spaced a distance  $d = 0.825$  apart. The vortex configurations are obtained by simulated annealing from a high temperature.

### III. RESULTS

In Fig. 1(b) we show the vortex configurations in the SF geometry for a system with  $d = 0.825$  at  $B/B_\phi = 1/2$ . Since the vortices are repulsive, they move as far away from each other as possible; however, when pinning is present, there is a competing pinning energy that favors having the vortices occupy the pinning sites. At  $B/B_\phi = 1/2$ , two neighboring pinning sites can be regarded as a single double well trap. An individual vortex can occupy one end of this double trap, determining the direction of the effective spin. The lowest energy per vertex would have two effective spins pointing “out” (away from the vertex) and two effective spins pointing “in” (toward the vertex); however, due to the geometric constraints, there must be some vertices with two spins in and one spin out, giving an energy higher than the ground state. A single cell in the SF ice contains four rectangular plaquettes that surround an inner

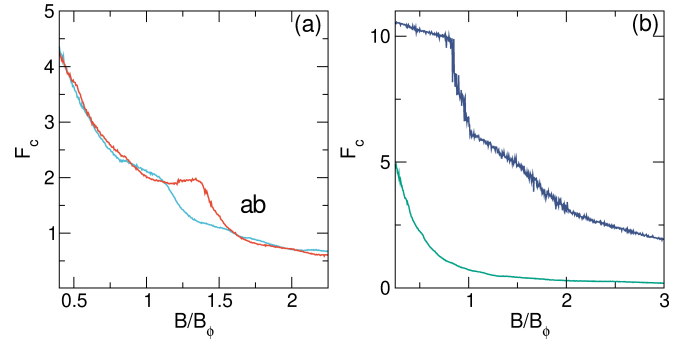


FIG. 2. (a) The critical depinning force  $F_c$  vs  $B/B_\phi$  for the SF system in Fig. 1(a) (blue curve) with  $d = 0.825$  and for a square pinning array (red curve). The matching field  $B_\phi$  is for the SF array; in these units, the matching field for the square array is at  $1.286B_\phi$ . The labels a and b indicate the value of  $B/B_\phi$  at which the images in Fig. 3 were obtained. (b) The critical depinning force  $F_c$  vs  $B/B_\phi$  for SF systems with different densities of  $d = 0.4$  (green curve) and  $d = 1.8$  (blue curve).

square. In Fig. 1(b), most of the vortices in the rectangular regions can form the two-out, two-in ground state; however, in the inner square there are several locations where two vortices are close together in neighboring pins, creating a high energy excitation. The overall configuration is close to the expected ice rule obeying state with forced excitations, as predicted for the magnetic version of the SF spin ice<sup>10,32</sup>. In Fig. 1(c) we illustrate the vortex configurations for  $B/B_\phi = 1.0$  at the commensurate field. Figure 1(d) shows the configurations at  $B/B_\phi = 1.5$ , where there are numerous instances of individual pinning sites capturing two vortices to form a vortex dimer state, along with several cases where vortices are located in the interstitial regions in the middle of the rectangular plaquettes. In this case, there is no long range order. For  $B/B_\phi = 2.0$  and  $2.5$  (not shown), the system remains disordered.

In Fig. 2(a) we plot the critical depinning force  $F_c$  which is proportional to the critical current as a function of  $B/B_\phi$  for the SF system in Fig. 1 and for a square pinning lattice. The  $x$  axis is normalized by the matching field  $B_\phi$  for the SF lattice, and in these units the matching field of the square lattice falls at  $1.286B_\phi$ . The square lattice exhibits a pronounced peak in  $F_c$  at the matching field similar to that found in other studies of vortex pinning on square substrates<sup>33,34</sup>. In the SF lattice, there is instead a broadened peak in  $F_c$  around the first matching field. For a square ice system at  $B/B_\phi = 1/2$ , previous work<sup>25</sup> has shown that a peak corresponding to the ice rule obeying ground state appears in the critical current that is as large as the matching peak at  $B/B_\phi = 1.0$ . For the SF array, there is no peak at  $B/B_\phi = 1/2$  due to the high energy excitations that are forced to exist by the SF geometry. Figure 2(a) shows that the overall pinning strength of the SF lattice is generally smaller than that of the square lattice due the fact that there are fewer pins; however, there are several regimes where the depinning force for the SF geometry is higher than that of the square array, particularly for  $B/B_\phi > 1.0$ . This is due to the tendency for the vortices in the square lattice to form easy flow one-dimensional channels along the sym-

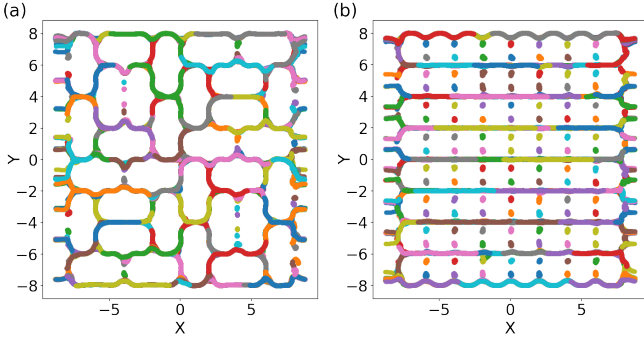


FIG. 3. The vortex trajectories for the system in Fig. 2(a) with  $d = 0.825$  at  $B/B_\phi = 1.67$ . (a) The SF lattice exhibits winding labyrinthine flow channels. (b) The square lattice has easy flow one-dimensional channels. The different colors correspond to different times.

metry axis of the pinning array. To more clearly illustrate this effect, in Fig. 3(a,b) we show the vortex trajectories at  $B/B_\phi = 1.67$  for the SF and square arrays, respectively, from Fig. 2(a) just above depinning. For the square array, the vortex motion follows one-dimensional interstitial channels between the vortices trapped at the pinning sites, while for the SF array, the motion occurs through a combination of longitudinal and transverse flow channels, so that some vortices move perpendicularly to the direction of drive at times. The results in Fig. 2(a) also imply that for an equivalent number of pinning sites, the SF lattice produces higher pinning than the square lattice.

In nanomagnetic spin ice systems, the ice rules are lost as the distance between the magnets is increased due to the reduction in the pairwise interactions between neighboring islands<sup>6</sup>. In the superconducting vortex system, the effective vortex interaction can be tuned by changing the distance between adjacent pinning sites. In Fig. 2(b) we plot the depinning force  $F_c$  versus  $B/B_\phi$  for two different pinning distances, the much larger value  $d = 1.8$  which corresponds to weak vortex interactions, and the much smaller value  $d = 0.4$  which produces strong vortex interactions. At  $d = 1.8$ , the vortices are far enough apart that the pinning dominates their dynamical behavior, and the overall depinning threshold is much higher. Additionally, there is no peak at  $B/B_\phi = 1.0$ , but instead there is a downward step in the critical current. In Fig. 4(a,b,c) we show the vortex configurations for the  $d = 1.8$  sample at  $B/B_\phi = 0.5, 1.5$ , and  $2.0$ . For  $B/B_\phi = 1/2$ , the vortex populations are random and do not form ice rule obeying states. For  $B/B_\phi = 1.5$  and  $2.0$ , there is a combination of doubly occupied sites and interstitial vortices. For a denser pinning lattice with  $d = 0.4$ , there are no peaks at  $B/B_\phi = 1/2$  or  $1.0$  and the overall pinning force is reduced. Since the pinning radius is fixed, at the smaller  $d$  the pinning sites begin to overlap, creating paths of low potential along which the vortices can flow, thereby reducing the effectiveness of the pinning. This also produces increasingly labyrinthine vortex configurations, as shown in Fig. 4(d,e,f) for  $B/B_\phi = 1/2, 1.5$ , and  $2.0$ . For higher fields at this value of  $d$ , the labyrinthine pattern persists. In an actual superconducting material in this

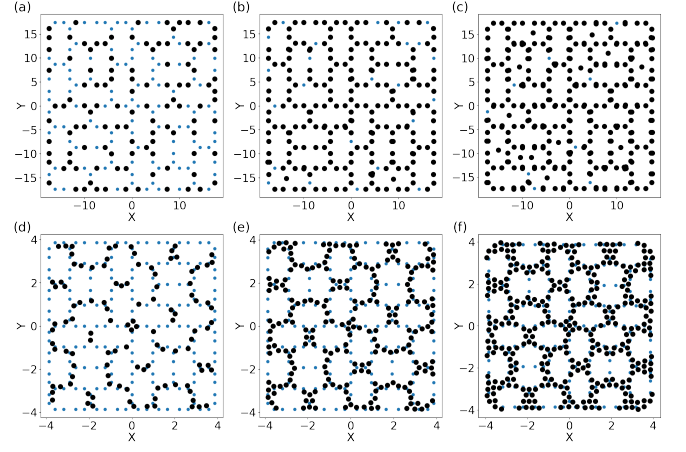


FIG. 4. (a,b,c) The pinning site locations (blue dots) and vortex positions (black dots) for the system in Fig. 2(b) at  $d = 1.8$  with weak vortex interactions where the ice rule is lost. (d,e,f) The same for the system in Fig. 2(b) with  $d = 0.4$ , where the pinning sites begin to overlap, creating labyrinthine vortex states. (a,d)  $B/B_\phi = 0.5$ . (b,e)  $B/B_\phi = 1.0$ . (c,f)  $B/B_\phi = 2.0$ .

regime, the vortices could merge to form multi-quanta states which would have to be studied using a model different than the point-like vortex model we consider here<sup>35</sup>.

#### IV. SUMMARY

We have numerically investigated vortex configurations, pinning and dynamics in a system with a Santa Fe artificial ice pinning site arrangement. This pinning geometry forces some vortices to occupy higher energy states. At half filling, the vortex configurations we observe are close to the ground state expected for the magnetic Santa Fe ice, with most of the vertices in low energy ice rule obeying states but with a small number of high energy vertices present. The critical depinning currents do not show a peak at the half matching field, but exhibit a rounded peak near the first matching field. For certain fillings, the Santa Fe ice has higher pinning than a square pinning array because the vortex flow in the Santa Fe ice runs both transverse and parallel to the driving direction, as opposed to the strictly parallel flow that occurs in the square array. For dense pinning arrays where the pinning sites begin to overlap, we find that the vortices can form an intricate labyrinthine state in the Santa Fe ice.

#### ACKNOWLEDGMENTS

We gratefully acknowledge the support of the U.S. Department of Energy through the LANL/LDRD program for this work. This work was supported by the US Department of Energy through the Los Alamos National Laboratory. Los Alamos National Laboratory is operated by Triad National Security, LLC, for the National Nuclear Security Administration of the U. S. Department of Energy (Contract No.

892333218NCA000001). WL and BJ were supported in part by NSF DMR-1952841.

Data available on request from the authors.

- <sup>1</sup>C. Nisoli, R. Moessner, and P. Schiffer, “Colloquium: Artificial spin ice: Designing and imaging magnetic frustration,” *Rev. Mod. Phys.* **85**, 1473–1490 (2013).
- <sup>2</sup>S. H. Skjærvø, C. H. Marrows, R. L. Stamps, and L. J. Heyderman, “Advances in artificial spin ice,” *Nature Rev. Phys.* **2**, 13–28 (2020).
- <sup>3</sup>L. Pauling, “The structure and entropy of ice and of other crystals with some randomness of atomic arrangement,” *J. Am. Chem. Soc.* **57**, 2680–2684 (1935).
- <sup>4</sup>P. W. Anderson, “Ordering and antiferromagnetism in ferrites,” *Phys. Rev.* **102**, 1008–1013 (1956).
- <sup>5</sup>S. T. Bramwell and M. J. P. Gingras, “Spin ice state in frustrated magnetic pyrochlore materials,” *Science* **294**, 1495–1501 (2001).
- <sup>6</sup>R. F. Wang, C. Nisoli, R. S. Freitas, J. Li, W. McConville, B. J. Cooley, M. S. Lund, N. Samarth, C. Leighton, V. H. Crespi, and P. Schiffer, “Artificial ‘spin ice’ in a geometrically frustrated lattice of nanoscale ferromagnetic islands,” *Nature (London)* **439**, 303–306 (2006).
- <sup>7</sup>J. P. Morgan, A. Stein, S. Langridge, and C. H. Marrows, “Thermal ground-state ordering and elementary excitations in artificial magnetic square ice,” *Nature Phys.* **7**, 75–79 (2011).
- <sup>8</sup>V. Kapaklis, U. B. Arnalds, A. Farhan, R. V. Chopdekar, A. Balan, A. Scholl, L. J. Heyderman, and B. Hjörvarsson, “Thermal fluctuations in artificial spin ice,” *Nature Nanotechnol.* **9**, 514–519 (2014).
- <sup>9</sup>E. Mengotti, L. J. Heyderman, A. F. Rodríguez, F. Nolting, R. V. Hügli, and H.-B. Braun, “Real-space observation of emergent magnetic monopoles and associated Dirac strings in artificial kagome spin ice,” *Nature Phys.* **7**, 68–74 (2011).
- <sup>10</sup>M. J. Morrison, T. R. Nelson, and C. Nisoli, “Unhappy vertices in artificial spin ice: new degeneracies from vertex frustration,” *New J. Phys.* **15**, 045009 (2013).
- <sup>11</sup>I. Gilbert, Y. Lao, I. Carrasquillo, L. O’Brien, J. D. Watts, M. Manno, C. Leighton, A. Scholl, C. Nisoli, and P. Schiffer, “Emergent reduced dimensionality by vertex frustration in artificial spin ice,” *Nature Phys.* **12**, 162 (2016).
- <sup>12</sup>Y.-L. Wang, Z.-L. Xiao, A. Snezhko, J. Xu, L. E. Ocola, R. Divan, J. E. Pearson, G. W. Crabtree, and W.-K. Kwok, “Rewritable artificial magnetic charge ice,” *Science* **352**, 962–966 (2016).
- <sup>13</sup>J. Drisko, T. Marsh, and J. Cumings, “Topological frustration of artificial spin ice,” *Nature Commun.* **8**, 14009 (2017).
- <sup>14</sup>Y. Perrin, B. Canals, and N. Rougemaille, “Extensive degeneracy, Coulomb phase and magnetic monopoles in artificial square ice,” *Nature (London)* **540**, 410 (2016).
- <sup>15</sup>A. Farhan, M. Saccone, C. F. Petersen, S. Dhuey, V. R. Chopdekar, Y.-L. Huang, N. Kent, Z. Chen, M. J. Alava, T. Lippert, A. Scholl, and S. van Dijken, “Emergent magnetic monopole dynamics in macroscopically degenerate artificial spin ice,” *Sci. Adv.* **5**, eaav6380 (2019).
- <sup>16</sup>C. Nisoli, V. Kapaklis, and P. Schiffer, “Deliberate exotic magnetism via frustration and topology,” *Nature Phys.* **13**, 200–203 (2017).
- <sup>17</sup>A. Ortiz-Ambriz, C. Nisoli, C. Reichhardt, C. J. O. Reichhardt, and P. Tierno, “Colloquium: Ice rule and emergent frustration in particle ice and beyond,” *Rev. Mod. Phys.* **91**, 041003 (2019).
- <sup>18</sup>A. Libál, C. Reichhardt, and C. J. O. Reichhardt, “Realizing colloidal artificial ice on arrays of optical traps,” *Phys. Rev. Lett.* **97**, 228302 (2006).
- <sup>19</sup>A. Ortiz-Ambriz and P. Tierno, “Engineering of frustration in colloidal artificial ices realized on microfeatured grooved lattices,” *Nature Commun.* **7**, 10575 (2016).
- <sup>20</sup>D. Y. Lee and P. Tierno, “Energetics and the ground state quest in an artificial triangular colloidal ice,” *Phys. Rev. Mater.* **2**, 112601 (2018).
- <sup>21</sup>A. Libál, D. Y. Lee, A. Ortiz-Ambriz, C. Reichhardt, C. J. O. Reichhardt, P. Tierno, and C. Nisoli, “Ice rule fragility via topological charge transfer in artificial colloidal ice,” *Nature Commun.* **9**, 4146 (2018).
- <sup>22</sup>A. Libál, C. Nisoli, C. J. O. Reichhardt, and C. Reichhardt, “Inner phases of colloidal hexagonal spin ice,” *Phys. Rev. Lett.* **120**, 027204 (2018).
- <sup>23</sup>F. Ma, C. Reichhardt, W. Gan, C. J. O. Reichhardt, and W. S. Lew, “Emergent geometric frustration of artificial magnetic skyrmion crystals,” *Phys. Rev. B* **94**, 144405 (2016).
- <sup>24</sup>A. Libál, C. J. O. Reichhardt, and C. Reichhardt, “Creating artificial ice states using vortices in nanostructured superconductors,” *Phys. Rev. Lett.* **102**, 237004 (2009).
- <sup>25</sup>M. L. Latimer, G. R. Berdiyrov, Z. L. Xiao, F. M. Peeters, and W. K. Kwok, “Realization of artificial ice systems for magnetic vortices in a superconducting MoGe thin film with patterned nanostructures,” *Phys. Rev. Lett.* **111**, 067001 (2013).
- <sup>26</sup>J. Trastoy, M. Malnou, C. Ulysse, R. Bernard, N. Bergeal, G. Faini, J. Lesueur, J. Briatico, and J. E. Villegas, “Freezing and thawing of artificial ice by thermal switching of geometric frustration in magnetic flux lattices,” *Nature Nanotechnol.* **9**, 710–715 (2014).
- <sup>27</sup>J.-Y. Ge, V. N. Gladilin, J. Tempere, V. S. Zharinov, J. Van de Vondel, J. T. Devreese, and V. V. Moshchalkov, “Direct visualization of vortex ice in a nanostructured superconductor,” *Phys. Rev. B* **96**, 134515 (2017).
- <sup>28</sup>Y.-L. Wang, X. Ma, J. Xu, Z.-L. Xiao, A. Snezhko, R. Divan, L. E. Ocola, J. E. Pearson, B. Jánko, and W.-K. Kwok, “Switchable geometric frustration in an artificial-spin-ice-superconductor heterosystem,” *Nature Nanotechnol.* **13**, 560 (2018).
- <sup>29</sup>X.-H. Chen, X.-D. He, A.-L. Zhang, V. V. Moshchalkov, and J.-Y. Ge, “Vortex ice pattern evolution in a kagome nanostructured superconductor,” *Phys. Rev. B* **102**, 054516 (2020).
- <sup>30</sup>Y.-Y. Lyu, X. Ma, J. Xu, Y.-L. Wang, Z.-L. Xiao, S. Dong, B. Jankó, H. Wang, R. Divan, J. E. Pearson, P. Wu, and W.-K. Kwok, “Reconfigurable pinwheel artificial-spin-ice and superconductor hybrid device,” *Nano Lett.* **20**, 8933–8939 (2020).
- <sup>31</sup>C. Nisoli, “Unexpected phenomenology in particle-based ice absent in magnetic spin ice,” *Phys. Rev. Lett.* **120**, 167205 (2018).
- <sup>32</sup>X. Zhang, A. Duzgun, Y. Lao, N. S. Bingham, J. Sklenar, H. Saglam, S. Subzwari, J. T. Batley, J. D. Watts, D. Bromley, C. Leighton, L. O’Brien, C. Nisoli, and P. Schiffer, “Excitation strings and topological surgery in artificial spin ice,” *arXiv e-prints*, arXiv:2008.07571.
- <sup>33</sup>M. Baert, V. V. Metlushko, R. Jonckheere, V. V. Moshchalkov, and Y. Bruynseraede, “Composite flux-line lattices stabilized in superconducting films by a regular array of artificial defects,” *Phys. Rev. Lett.* **74**, 3269–3272 (1995).
- <sup>34</sup>C. Reichhardt, J. Groth, C. J. Olson, S. B. Field, and F. Nori, “Spatiotemporal dynamics and plastic flow of vortices in superconductors with periodic arrays of pinning sites,” *Phys. Rev. B* **54**, 16108–16115 (1996).
- <sup>35</sup>K. Tanaka, I. Robel, and B. Janko, “Electronic structure of multiquantum giant vortex states in mesoscopic superconducting disks,” *Proc. Natl. Acad. Sci. (USA)* **99**, 5233–5236 (2002).